# View-dependent compression of digital hologram based on matching pursuit

Anas El Rhammad, Patrick Gioia, Antonin Gilles, Marco Cagnazzo, Béatrice Pesquet-Popescu

Anas El Rhammad, Patrick Gioia, Antonin Gilles, Marco Cagnazzo, Béatrice Pesquet-Popescu, "View-dependent compression of digital hologram based on matching pursuit," Proc. SPIE 10679, Optics, Photonics, and Digital Technologies for Imaging Applications V, 106790L (24 May 2018); doi: 10.1117/12.2315233

SPIE.

Event: SPIE Photonics Europe, 2018, Strasbourg, France

# View-dependent compression of digital holograms based on matching pursuit

Anas El Rhammad[1,3], Patrick Gioia[1,2], Antonin Gilles[1], Marco Cagnazzo[1,3], and Béatrice Pesquet-Popescu[3]

[1]Institute of Research & Technology b-com, 35510 Cesson-Sévigné, France
[2]Orange Labs, 35510 Cesson-Sévigné, France
[3]LTCI, Télécom ParisTech, Université Paris-Saclay, 75013, Paris, France

## ABSTRACT

In this paper we investigate the suitability of Gabor Wavelets for an adaptive partial reconstruction of holograms based on the viewer position. Matching Pursuit is used for a sparse light rays decomposition of holographic patterns. At the decoding stage, sub-holograms are generated by selecting the diffracted rays corresponding to a specific area of visualization. The use of sub-holograms has been suggested in the literature as an alternative to full compression, by degrading a hologram with respect to the directional degrees of freedom. We present our approach in a complete framework for color digital holograms compression and explain, in details, how it can be efficiently exploited in the context of holographic Head-Mounted Displays. Among other aspects, encoding, adaptive reconstruction and selective degradation are studied.

**Keywords:** Digital holography, Gabor wavelets, Compression, Matching Pursuit, Adaptive reconstruction

## 1. INTRODUCTION

Digital holography is considered as a very appealing technology for immersive visual applications and a promising alternative to compete with (auto)-stereoscopic devices or sparsely distributed multiview.[1] Indeed, holography has the ability to render exact continuous parallax and accommodation distance by providing all depth perception cues without any eye-strain.[2] However, this technology has long been considered as immature for general public applications because of the resolutions and pixel size needed for TV-like displays, that remain out of reach by today's LCD technology.

With the recent wide interest for Head-Mounted Displays (HMD) applied to Virtual or Augmented Reality (VR or AR), holography could find a short term application context that perfectly suits both its advantages and requirements: on the one hand holographic representation of real or virtual scenes is the ideal solution to the uncomfortable experience provided by stereoscopic HMDs and caused by the accommodation / vergence mismatch.[3] On the other hand, all that was a handicap so far, namely the small size of the displays and restricted viewing angle do meet the requirements of miniaturization of HMDs and the necessity to restitute the perspective for only one viewpoint.

For such application, the reconstructed hologram only depends on the position and orientation of the observer; hence, from a representation point of view, it might be interesting to deal with data formats that are suited to real-time adaptation of a global holographic scene into a specific reconstruction corresponding to the viewing conditions at a given time. This would allow to reduce, significantly, the amount of information to reconstruct and display, and possibly to transmit.

The seminal approach for such representation was proposed by SeeReal.[4–7] In,[7] a holographic display prototype based on the adaptation to the viewing window of an observer is presented. The minimal relevant features are gathered in partial reconstructions called sub-holograms. However, those are mostly pre-computed according to clustered directional features. In order to allow precise view-dependent selection of data to reconstruct into

Authors can be reached at: {anas.elrhammad, patrick.gioia, antonin.gilles}@b-com.com & {cagnazzo, beatrice.pesquet}@telecom-paristech.fr

the displayed hologram, the representation should be based on a concise extraction of the directional information locally present in the hologram.

In this context, an approach that might be of interest but which is still relatively little studied is the expansion of holograms in a basis of functions that may not guarantee optimal compression but instead are able to precisely analyze the local frequencies of the hologram features.[8] Such decomposition has the advantage to provide a real-time generation of sub-holograms based on the position and viewing direction of the observer.

Digital holograms typically contain a tremendous amount of data corresponding to a continuum of perspectives with arbitrary depth. This large set of data is represented as 2D complex patterns since it carries amplitude and phase information of the light wave scattered by the object across a 2D surface. Thus, the first trivial attempts to compress holographic contents consisted in applying image compression methods.[9–12] Despite the practical use and efficiency of such algorithms for image compression, they are still lacking high compression rate for digital hologram coding. Therefore, it is not surprising that more elaborated techniques are needed,[13] the information being organized in a completely different way from semantically meaningful images: a hologram is the superposition of very high frequency components, which have to be analyzed by specific tools. Among those, several types of wavelets were proposed. In,[14,15] a basis of Fresnelet wavelets is used by the authors to decompose the complex wavefield. The obtained coefficients are then encoded using the Set Partitioning in Hierarchical trees[16] (SPIHT). Despite the significant compression gain achieved by this approach, the compression does not consider the adaptive functionalities[17] and depends on the reconstruction distance of the hologram. Recently, the use of Gabor / Morlet wavelets was proposed to analyze and reconstruct sub-holograms in a view-dependent context.[8,18] Although the theoretical aspects of this approach and its possible network implementation were presented, no realistic visual evaluation nor significant compression results were reported. In our previous work, we proposed a novel method for a sparse Gabor expansion of digital holograms based on Matching Pursuit.[19] The compression aspects of this approach were deeply studied with an objective and visual evaluation of the reconstructed holograms. However, our study did not take into account the constraints related to the observer conditions.

Accordingly, in this paper, we propose an extension of our previous approach in an adaptive view-dependent context where a single viewer may have several points of view, for example in a AR application. Gabor wavelets are used to model the light rays diffracted by hologram patterns. Matching Pursuit is applied for a sparse representation of the wavelets coefficients. Then, the adaptive selection (AS) is performed based on the viewer's position and orientation. We establish the strategy of coefficient pruning, evaluate the visual degradation caused by wavelet coefficients selectivity, and present the overall compression rates.

The rest of the article is structured as follows: in Section 2, the view-dependent setting is introduced and linked to the properties of the retained wavelets in a user case. Then, in Section 3, the directional character of Gabor wavelets and the pruning process is exposed for a real-time generation of sub-holograms. The process of generating a sparse Gabor decomposition using Matching Pursuit as well as the overall compression consideration are briefly presented in section 4. Experimental results are shown in Section 5 and compared to our previous approach and the H.265 codec.

## 2. OVERVIEW

The basic idea consists in expanding the original hologram according to a set of analyzing wavelets whose intrinsic properties match the way information is organized inside the patterns; hence this set of functions may not be optimal in terms of compression, i.e. it may not lead to the sparsest representation when considering the hologram in its entirety. However, to allow adaptive view-dependent reconstruction, it should provide a convenient way to generate a sub-hologram corresponding to the viewer's position.

Figure 1 shows the typical applicative setup for a networked implementation of our approach. First of all, an overcomplete set with $N$ coefficients $\{c_n\}_{1\leq n\leq N}$ is produced by decomposing the target hologram $\mathbf{H}$ through a complex Gabor dictionary $D$. Then, a subset $\{c_k\}_{1\leq k\leq K}$ is obtained from the overcomplete set $\{c_n\}$ using Matching Pursuit K-expansion, where $K < N$. This subset is computed offline and stored in the server. When the user position is updated, the viewing parameters are computed using an eye-tracking system[20] and sent to the server through a backchannel. Then, an adaptation module selects the subset $\{c_m\}^V_{1\leq m\leq M}$, corresponding to

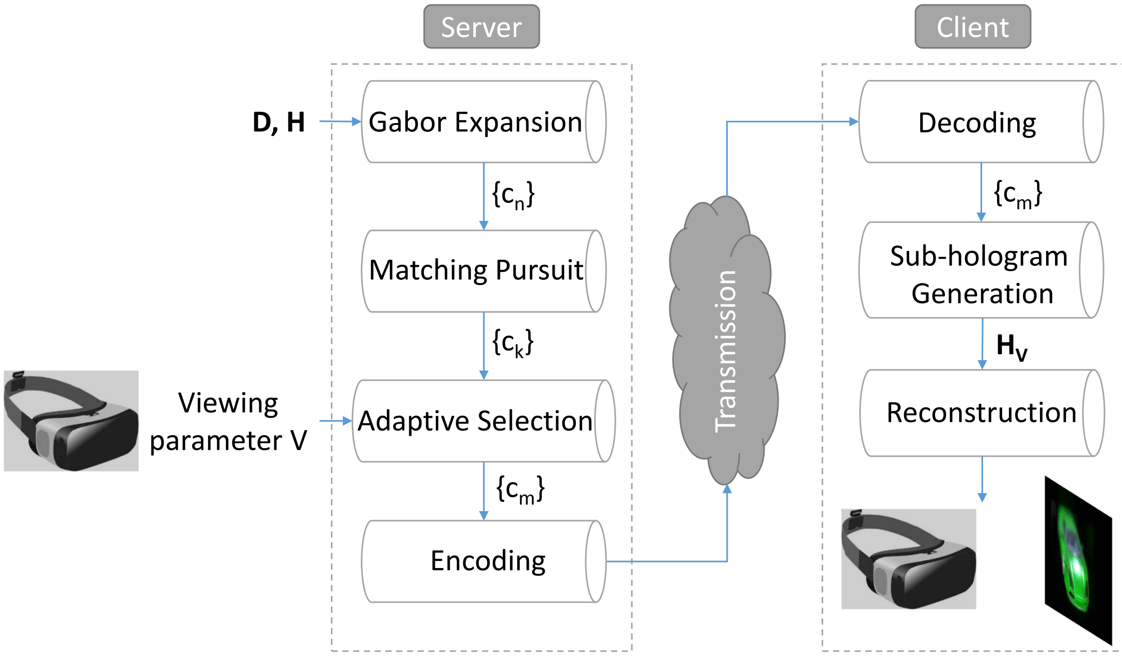


Figure 1: User-case diagram of hologram adaptive transmission

the current point of view $V$ where $M < K$, from the available wavelet coefficients previously stored. The selected coefficients are further quantized and efficiently encoded. Once the bitstream is generated, it is transmitted to the client for decoding and the associated sub-hologram $\mathbf{H_V}$ is then retrieved. Finally, $\mathbf{H_V}$ is displayed on the HMD using a Spatial Light Modulator (SLM).[21] In order to prevent any lag, a larger viewing window can be considered, so as to anticipate the observer movements that may have occurred between the request and the reception of the coefficients.

The present study focuses on the generation of a suitable subset of wavelet coefficients which meets the following requirements:

- Fast coefficients selection: the relation between the coefficients and the viewing parameters should be straightforward to avoid intensive computations during visualization.
- Faithful sub-hologram reconstruction: the degradation induced by the selection of coefficients should not significantly impact the image quality within the viewing window.
- Reasonable compression: although the reduction of the amount of transmitted data is sought from the coefficients pruning, an efficient encoder is required to allow an online transmission. A measure of the compressibility can be evaluated by the overall hologram compressed size.
- Reducing the impact of seeking the sparsest representation: choosing wavelets providing good tradeoff between space and frequency localization guarantees to identify the diffraction properties of the hologram, but leads to a large choice of possible representations, some of which may not visually preserve the directional information.

In the next section we exploit the anisotropic character of Gabor wavelets to extract the directional information of diffracted light rays. We also explain the process of sub-holograms generation based on the directional Gabor decomposition in a view-dependent context.

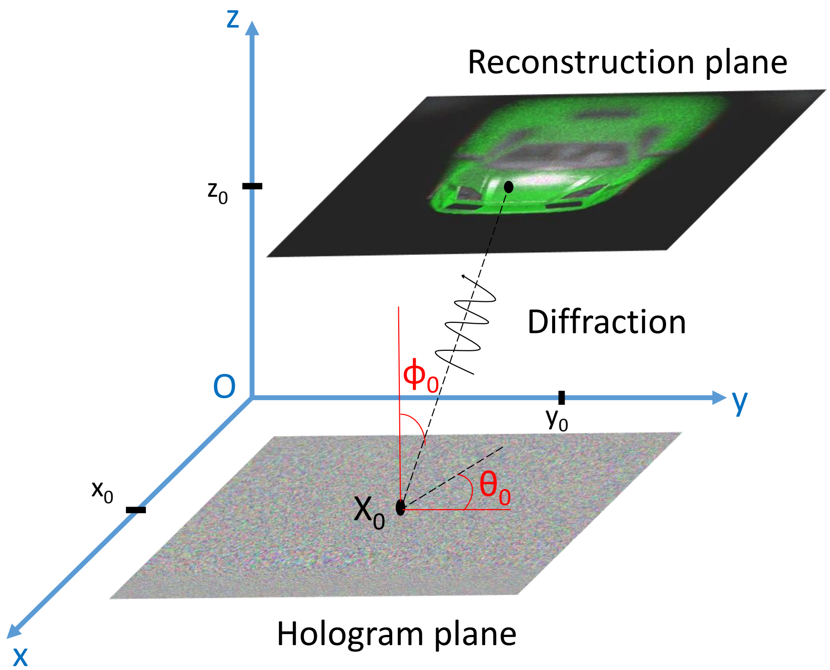


Figure 2: Ray light diffraction in spherical coordinates

## 3. GABOR WAVELETS FOR REAL-TIME SUB-HOLOGRAMS GENERATION

To extract sub-holograms corresponding to the viewer's position on the fly, one has to establish a formal relation between the directional information of light diffracted by the hologram and the properties of the transform.

### 3.1 Duality between Gabor wavelets and light rays

The diffractive behavior of a hologram depends on the frequencies locally present in the considered pattern; hence a hologram can be considered as the superimposition of infinitesimal diffraction gratings. The dependency between the diffraction angle $\phi$ of a light ray and its corresponding spatial frequency $f$ is given by the grating equation[22]

$$f = \frac{\sin(\phi)}{\lambda}, \tag{1}$$

where $\lambda$ is the wavelength of the diffracted light.

Let us consider a 2D frequency $\mathbf{f_0} = (f_{x_0}, f_{y_0})$ that is present at location $\mathbf{X_0} = (x_0, y_0)$ in the hologram, where $f_{x_0}$ and $f_{y_0}$ denote the spatial frequencies in directions $x$ and $y$, respectively. A light ray incident at $\mathbf{X_0}$ is diffracted in the direction given by polar and azimuthal angles

$$(\theta_0, \phi_0) = \left(\arctan 2(f_{x_0}, f_{y_0}), \arcsin\left(\lambda\sqrt{f_{x_0}^2 + f_{y_0}^2}\right)\right), \tag{2}$$

as shown in Figure 2.

Aiming for an accurate light-ray decomposition of the hologram, it is thus necessary to have a good space / frequency analysis, providing the best localization trade-off in both domains. Hence a better localization in space will lead to better precision in finding $\mathbf{X}$ position, and a better frequency localization will narrow down the angular uncertainty on the ray direction.

Among various windowed basis functions, Gabor wavelets are known to provide the best possible localization in both space and frequency.[23] In their original 2D form these functions are the product of a complex sinusoid and a Gaussian

$$\psi(\mathbf{X}) = e^{-\frac{||\mathbf{X}||^2}{2}} e^{i2\pi\mathbf{X}\cdot\mathbf{f}}, \tag{3}$$

where $\mathbf{f} = (f_x, f_y)$ is the 2D frequency of the sinusoid.

Then, for a given hologram $h : \mathbb{R}^2 \rightarrow \mathbb{C}$, the Continuous Wavelet Transform associated to Gabor Wavelets is defined as

$$Wh(\theta, s, \mathbf{t}) = \frac{1}{\sqrt{s}} \int_{\mathbf{R}^2} d\mathbf{X} h(\mathbf{X}) \psi\left(R^{-\theta}\left(\frac{\mathbf{X}-\mathbf{t}}{s}\right)\right), \tag{4}$$

where $\mathbf{t}$ is the shift vector, $R^{-\theta}$ the rotation matrix and $s > 0$ the frequency dilation parameter.

Accordingly, the relation between a light ray $(\mathbf{X}_0, \theta_0, \phi_0)$ diffracted by a hologram and a Gabor wavelet with parameters $(\theta, s, \mathbf{t})$ is given by the following equivalence

$$\begin{cases} \mathbf{X}_0 = \mathbf{t} \\ \theta_0 = \theta \\ \phi_0 = \arcsin\left(\dfrac{\lambda f}{s}\right). \end{cases} \tag{5}$$

Inversely, the original hologram $h$ can be recovered by the inverse transform

$$h(\mathbf{X}) = \int_0^{\infty} \int_0^{2\pi} \int_{\mathbf{R}^2} Wh(\theta, s, \mathbf{t}) \psi\left(R^{-\theta}\left(\frac{\mathbf{X}-\mathbf{t}}{s}\right)\right) ds d\theta d\mathbf{t}. \tag{6}$$

In fact, the set $\{\psi_{\theta,s,\mathbf{t}}\}$ with continuously varying parameters $s$, $\mathbf{t}$ and $\theta$ is extremely redundant and many other functions can replace $Wh(\theta, s, \mathbf{t})$ in Eq. (6) so that the equality still holds. One way to reduce this redundancy is to suitably discretize parameters $s$, $\mathbf{t}$ and $\theta$ so that we end up with a discrete transform with a set of functions that tend to form an actual basis. We define in Section 3.2 the discrete Gabor wavelets in their 2D form, and we explain how the duality of Eq. (5) can be exploited for a sub-hologram generation through an adaptive selection.

### 3.2 Sub-hologram generation process

The main advantage of Gabor wavelets for the extraction of sub-holograms corresponding to the viewer's position is their accurate localization in both space and frequency domains. As a consequence, to take advantage of this property, the discretization of Gabor wavelets should be dense enough since any sparsification of the parameters $s$, $\mathbf{t}$ and $\theta$ directly implies a loss on continuity in the directions of diffracted rays. In the rest of the article, we assume that the dilation and orientation parameters are densely discretized with $L$ and $P$ levels, respectively, and defined by

$$\begin{cases} s[l] = 2^{\alpha(l)} \\ \theta[p] = \dfrac{p\pi}{P}, \end{cases} \tag{7}$$

where the integers $l$ and $p$ are the indexes of discretization corresponding to $s$ and $\theta$, respectively. $\alpha$ is an arbitrary linear function.

The discrete Gabor wavelets $\widetilde{\psi}_{(l,p)}$ in their 2D form are thus given by

$$\widetilde{\psi}_{(l,p)}[u, v] = \frac{1}{\sqrt{s[l]}}\ e^{-\frac{1}{2s[l]^2}(a^2+b^2)}\ e^{i2\pi a\frac{f_{max}}{s[l]}}, \tag{8}$$

where

$$\begin{cases} a = u\cos(\theta[p]) + v\sin(\theta[p]) \\ b = v\cos(\theta[p]) - u\sin(\theta[p]). \end{cases} \tag{9}$$

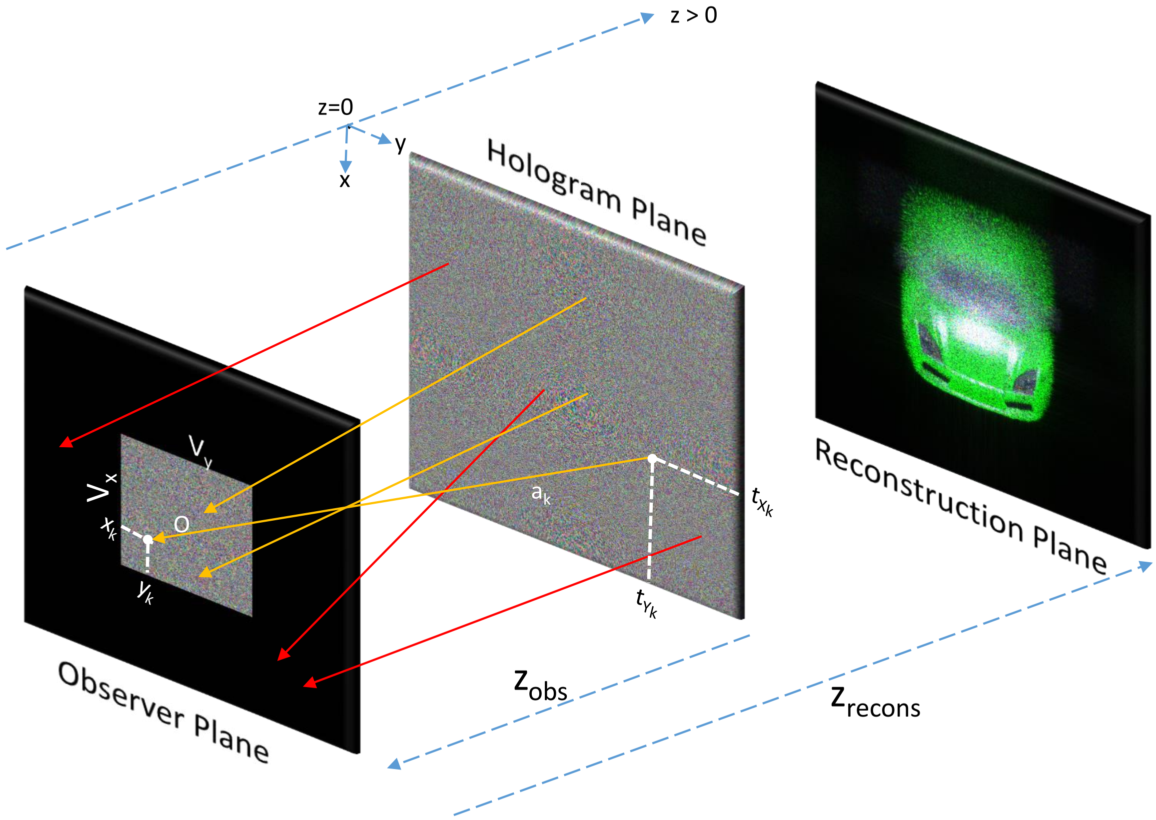


Figure 3: Adaptive selection and reconstruction scheme

In Eq.(8), $(u, v) \in \mathbb{Z}^2$ is the 2D shift discretized parameter such that: $-\frac{M_x}{2} \leq u < \frac{M_x}{2}$ and $-\frac{M_y}{2} \leq v < \frac{M_y}{2}$, where $(M_x, M_y)$ is the wavelet resolution. The frequency of the Gabor function is defined by $f_{max} = (2\Delta)^{-1}$, where $\Delta$ is the pixel pitch of the hologram.

We denote by $(N_x, N_y)$ the spatial resolution of the discrete hologram $\mathbf{H}$. An overcomplete N-expansion $\{\mathbf{c}_n\}_{1 \leq n < N}$ of $\mathbf{H}$, where $N = N_x N_y LP$, is the set of its Gabor coefficients. It is generated by computing the inner-product values $\{\langle \mathbf{H}, \widetilde{\psi}_{(l,p)} \rangle\}_{\substack{1 \leq l \leq L \\ 1 \leq p \leq P}}$.

Although the set of wavelets coefficients $\{\mathbf{c}_n\}_{1 \leq n < N}$ enables a space/frequency decomposition of hologram patterns, it may not lead to the sparsest representation in terms of compression, since it provides an overcomplete representation. Therefore, and as mentioned in Section 2, the N-expansion is reduced to a set of only $K$ coefficients using the Matching Pursuit algorithm. The summary of this technique is presented in the next section.

Let us now assume that such sparse K-expansion $\{\mathbf{c}_k\}_{1 \leq k < K}$ is generated. $A_K$ denotes the set of $K$ Gabor atoms where the $k^{th}$ element is given by

$$a_k = (c_k, l_k, p_k, \mathbf{t}_k). \tag{10}$$

As aforementioned, each atom $a_k$ represents a light ray diffracted from a position $\mathbf{t}_k$ in direction

$$(\phi_k, \theta_k) = (\phi(s[l_k]), \theta[p_k]). \tag{11}$$

The adaptive pruning and reconstruction process for a given point of view $V$ is explained in Figure 3: the observer position is denoted by $O(O_x, O_y, O_{z_{obs}})$, the viewing window dimensions are $V_x$ and $V_y$ in directions $x$ and $y$ respectively, the hologram plane is located at $z = 0$ whereas the reconstruction plane is located at $z = z_{recons}$. We seek to extract from $\mathbf{H}$ the sub-hologram $\mathbf{H_V}$ such that every light ray diffracted by $\mathbf{H_V}$ passes through the viewing window $V$. To this end, for every ray represented by $a_k \in A_k$, we compute the coordinates $(x_k, y_k)$ of the point through which the ray intersects the observer plane.

Then a subset $A_M^V$ of $A_K$ with $M < K$ atoms can be extracted as

$$A_M^V = \{a_k \in A_K \quad | \quad (x_k, y_k) \in V, 1 \leq k \leq K\}. \tag{12}$$

The $m^{th}$ atom of $A_M^V$ thus corresponds to a ray which passes through the viewing window $V$. In Figure 3, the rays passing through the viewing window $V$ are represented in yellow, whereas others are represented in red.

Experimentally, we will verify in Section 5 that the sub-hologram $\mathbf{H_V}$ and original hologram $\mathbf{H}$ produce the same reconstruction at considered viewpoint.

## 4. MATCHING PURSUIT AND COMPRESSION CONSIDERATION

As stated before, the set of Gabor coefficients $\{\mathbf{c}_n\}_{1\leq n<N}$ form an overcomplete representation allowing one possible recovery of the hologram $\mathbf{H}$, but such solution may not be the optimal in terms of sparsity. Aiming at generating a compressed bitstream for a real-time transmission, it is common to search for the sparsest expansion, i.e. the set of wavelet coefficients that has a maximum number of vanishing entries. For this, a well-known algorithm is the so-called *Matching Pursuit*[24] (MP).

In Section 4.1, we emphasise the use of the MP algorithm for digital holograms to obtain a K-expansion $\{\mathbf{c}_k\}_{1\leq k<K}$ where $K < N$. Then, a summary of the overall quantification and encoding choices is presented in Section 4.2 for an efficient compression of the pruned subset $A_M^V$ corresponding to sub-hologram $\mathbf{H_V}$.

### 4.1 Matching Pursuit algorithm

Matching pursuit is a greedy algorithm applied to signal retrieval from redundant dictionary. It is widely used in several domains such as image denoising,[25] video coding,[26] compressed sensing.[27] MP allows a linear expansion by greedily selecting from a dictionary the atoms that provide maximum correlation with the target signal. Thus, a wise choice of these atoms may improve the reconstruction accuracy, as well as the convergence speed to an optimal solution. As shown in Section 3.1, Gabor functions are a good choice to match the hologram patterns due to their accurate space/frequency localization.

Correspondingly, we build a complex dictionary $D$ with the 2D discrete Gabor wavelets $\widetilde{\psi}_{(l,p)}$ as defined in Eq. 8 and having unit norm. The MP algorithm is given in Algorithm 1, where the atom index $\gamma_k = (l_k, p_k, \mathbf{t}_k)$ maximising the inner-product values is extracted, and each residual $R_k(\mathbf{H})$ is then updated.

**Algorithm 1:** MP

**Input :** Hologram $\mathbf{H}$, Dictionary $D$
**Output:** atom coefficients $\{c_k\}$ and indexes $\{\gamma_k\}$
Initialization: $R_0(\mathbf{H}) = \mathbf{H}$
**for** $k \in \{1, \ldots, K\}$ **do**
  $\gamma_k = \arg\max_{\gamma} |\langle R_k(\mathbf{H}), \widetilde{\psi}_{(l,p)}\rangle|$
  $c_k = \langle R_k(\mathbf{H}), \widetilde{\psi}_{(l_k,p_k)}\rangle$
  Update : $R_{k+1}(\mathbf{H}) = R_k(\mathbf{H}) - c_k\widetilde{\psi}_{(l_k,p_k)}$
**end**

Inversely, MP allows a hologram recovery from the K extracted atoms through the linear approximation

$$\hat{\mathbf{H}} = \sum_{k=0}^{K} c_k \widetilde{\psi}_{(l_k,p_k)}. \tag{13}$$

### 4.2 MP encoder

For transmission purposes, a compressed bitstream should be generated from the $M$ atoms corresponding to the light rays diffracted by the sub-hologram $\mathbf{H_V}$. To this end, the statistical properties, the encoding order and format of MP components (i.e. the coefficients and the indexes) should be analysed to optimise the trade-off between the total coding rate and the distortion of the reconstructed view.

The bitstream $B$ that encodes the subset $A_M^V$ obtained by the adaptive selection process, presented in Section 3.2, is given by

$$B = \{([c_m], l_m, p_m, \mathbf{t}_m); \qquad 1 \leq m \leq M\}, \tag{14}$$

where $[c_m]$ is the quantized value of $c_m$ .

The main design choices for the MP encoder were deeply studied in our previous works[19] and are summarized here:

- **Coding order:** encoding atom coefficients in the decaying order of their magnitude is very costly since $\log_2(N_x) + \log_2(N_y)$ bits are needed for each position. Thus, an alternative is to represent them in a raster-scan order where each 2D position $\mathbf{t}_m$ is represented by

$$\delta_m = [t_{x_m} + (N_x - 1) \cdot t_{y_m}] - [t_{x_{m-1}} + (N_x - 1) \cdot t_{y_{m-1}}]. \tag{15}$$

  Then, the differential position $\delta_m$ is encoded using a context-based arithmetic encoder with a two-neighbours context.

- **Dilation indexes:** it has been found that using an arithmetic encoder without context is efficient for encoding the set $\{l_k\}$ since we obtain a 24% bit rate reduction over the fixed length code.

- **Rotation indexes:** applying an arithmetic encoder to encode the set $\{p_k\}$ shows that no gain can be achieved, so it is encoded with a fixed length code using $\log_2 P$ bits.

- **MP coefficients:** are quantized using a uniform quantizer (UQ) with a number of bits which depends on the target bit rate. Then, the quantized coefficients are represented as real and imaginary part, and each of them is encoded using a context-based arithmetic encoder with a 1D two-neighbours context.

In the next section, we will verify, experimentally, if the MP sparse representation preserves the adaptive reconstruction properties previously mentioned. Indeed, the fact that the K-expansion leads to the same reconstruction as the one obtained by the N-expansion doesn't straightforwardly imply that a partial reconstruction would still contain the necessary directional information. Moreover, we report the compression performance obtained by our approach.

## 5. EXPERIMENTAL RESULTS

In this section we evaluate the effectiveness of the proposed method to compress digital holograms. The target of hologram compression is not to preserve the complex hologram signal but rather the quality of the reconstructed image. Therefore, in all our experimental tests we use as quality metric the PSNR between two images: the one reconstructed from the original hologram, and the one reconstructed from the compressed hologram. The cost metric is the total rate needed to encode the holographic signal. To validate our approach, and for simplicity purposes, three different points of view are considered: top left, central and right.

It is judicious to note that the approach proposed in this work is relevant for both types of digital holograms: *optically acquired holograms* and *computer-generated holograms* (CGHs). Since they are easier to acquire, CGHs will be considered for the simulations results.

Therefore, we use two color CGHs ($\mathbf{H}_1$ : Diffuse Car, $\mathbf{H}_2$ : Ring) with a $4096 \times 4096$ resolution and a pixel pitch $\Delta = 0.4$µm.[28] The parameters of $\mathbf{H}_1$ and $\mathbf{H}_2$ are given in our holographic repository.[29]

Table 1 summarizes the observer parameters for the three considered points of view. These values are given in accordance with the system coordinates defined in Figure 3.

Table 1: Observer parameters

| View | Parameter | | | | | |
|---|---|---|---|---|---|---|
| | $O_x$ (mm) | $O_y$ (mm) | $z_{obs}$ (mm) | | $z_{recons}$ (mm) | |
| | | | $\mathbf{H}_1$ | $\mathbf{H}_2$ | $\mathbf{H}_1$ | $\mathbf{H}_2$ |
| *Central* | 0.82 | 0.82 | -0.83 | -1.22 | 2.02 | 2.81 |
| *Right* | 1.22 | 0.82 | -0.62 | -0.91 | 1.81 | 2.5 |
| *Top left* | 0.41 | 0.41 | -0.5 | -0.73 | 1.69 | 2.32 |

The partial reconstruction $\mathbf{R_V}$ corresponding to the view $V$ is obtained by propagating the cropped wavefield in the observer plane to the reconstruction plane. $\mathbf{R_V}$ is given by

$$\mathbf{R_V} = \mathcal{F}_{z_{recons}}(\mathcal{F}_{z_{obs}}(\mathbf{H_V})), \tag{16}$$

where $\mathcal{F}_z(\cdot)$ is the propagation operator for a distance $z$.

The viewing window dimensions are given by $(V_x, V_y)$. To reduce the speckle effect in numerical reconstruction, a large cropping window should be considered. In our experiments, we use $(V_x, V_y) = (0.64mm, 0.64mm)$ for both holograms.

To evaluate our approach, we compare the rate distortion (RD) graphs corresponding to the numerical reconstructions obtained from:

- The sub-hologram $\mathbf{H_V}$ computed using the Matching Pursuit plus Adaptive Selection (MP+AS).
- The complete hologram encoded using Matching Pursuit encoder (MP-only).
- The complete hologram encoded using HEVC codec in intra-mode.

The RD graphs obtained by MP+AS, MP-only and HEVC for the three considered reconstructed views of $\mathbf{H}_1$ and $\mathbf{H}_2$ are presented in Figure 4 and Figure 5, respectively.

As shown in RD graphs, our approach clearly outperforms HEVC in terms of compression performance for the right and top left views at different bit rates and for the central view especially in medium and high bit rates. Moreover, a significant gain is achieved by the MP+AS expansion compared to the MP-only one for a given quality reconstruction, since less atoms are encoded. Table 2 summarizes the atoms reduction ratio $(1 - \frac{M}{K})$, as well as the compression gain $(1 - \frac{R_{MP+AS}}{R_{MP-only}})$ obtained for a reference PSNR value $P_{ref} = 34.8$dB.

As shown in Table 2, the bit rate gains achieved by the pruning process depend on the considered point of view. For the same reconstruction quality, a compression gain of 45.8% is attained for the top left view of $\mathbf{H}_1$ compared to the MP-only expansion.

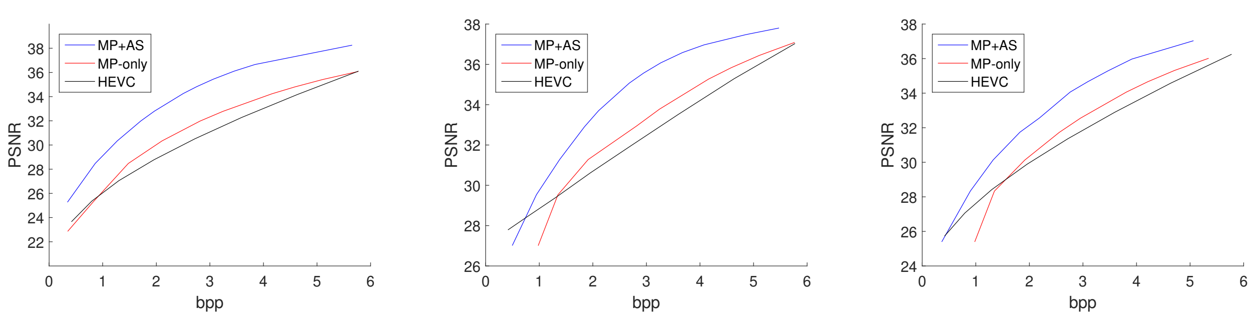


(a) (b) (c)

Figure 4: RD graphs for numerical reconstruction of $\mathbf{H}_1$: (a) Top left view, (b) central view, (c) right view

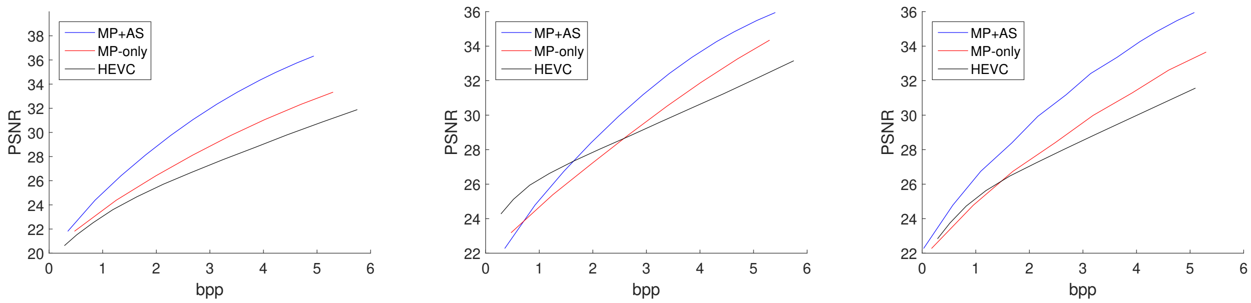


(a) (b) (c)

Figure 5: RD graphs for numerical reconstruction of $\mathbf{H}_2$ : (a) Top left view, (b) central view, (c) right view

Table 2: Comparison of MP+AS and MP-only expansion: Atoms reduction and corresponding bit rate gains

| | $\mathbf{H}_1$ | | | $\mathbf{H}_2$ | | |
|---|---|---|---|---|---|---|
| | *Central* | *Right* | *Top left* | *Central* | *Right* | *Top left* |
| Atoms reduction ($\in [0, 1]$) | 0.41 | 0.35 | 0.46 | 0.26 | 0.37 | 0.39 |
| Bit rate gain (%) | 36.4 | 26.8 | 45.8 | 17.7 | 29.3 | 33.4 |

To confirm the objective compression results obtained by the RD graphs, the three reconstructed views corresponding to $\mathbf{H}_1$ and $\mathbf{H}_2$ are presented in Figures 6 and 7, respectively. The top left views are shown in the first column, the central views in the second one and the right reconstructions in the third columns. The bit rates of the compressed CGHs $\mathbf{H}_1$ and $\mathbf{H}_2$ are $bpp_1 = 2.76$ and $bpp_2 = 2.65$, respectively.

For all reconstructed views, MP+AS expansion presents a better visual quality than HEVC and MP-only expansion which confirms the RD results. For instance, when considering the diffuse-car reconstruction from the right point of view, a gain of 2.7dB is reached by the pruning selection compared to HEVC, where only 0.7dB is achieved without the adaptive selection process. For the top left reconstruction of the ring CGH, the PSNR values was found to be 31.1dB for MP+AS expansion, 28.1dB for MP-only one and 26.6dB for HEVC. Thus, the proposed method provides a good reconstruction quality with a high compression rate.

Based on the aforementioned experimental simulations, we conclude that the sparse MP representation does not affect the adaptive reconstructions properties developed in Section 3.2. The sub-holograms generated by the combination of MP and AS provide a good reconstruction quality with significant compression gains.

## 6. CONCLUSION

In this paper, we studied the use of Gabor wavelets for an accurate space/frequency decomposition of hologram patterns and their suitability for a partial reconstruction based on the viewer position. The generation of compressed sub-holograms in a view dependent context is conducted through two stages: first, the overcomplete Gabor expansion is reduced to a sparse set of atoms using matching pursuit. Then, an adaptive selection based on the observer position enables a pruning of a subset with only the atoms modeling the light rays passing through the viewing window.

Experimental results revealed that the sparse sub-holograms generated by combining MP and AS provide the same reconstruction quality as the entire hologram. Compared to the uncompressed representation, a compression ratio of 48 : 2.3 is achieved by our approach, 48 : 3.1 for the MP-only version and 48 : 3.6 for HEVC used in intra-mode. Moreover, the straightforward correspondence between the localisation parameters of Gabor wavelets and the directions of diffraction may be exploited for a real-time progressive transmission in the future works.

## ACKNOWLEDGMENTS

This work has been completed within the Institute of Research and Technology b¡¿com. It has been supported by the French government through the National Research Agency (ANR) Investment referenced ANR-A0-AIRT-07.

## REFERENCES


[1] Dufaux, F., Pesquet-Popescu, B., and Cagnazzo, M., eds., [*Emerging Technologies for 3D Video: Creation, Coding, Transmission and Rendering*], John Wiley & Sons, Ltd (2013).

[2] Schnars, U. and Jüptner, W., [*Digital Holography: Digital Hologram Recording, Numerical Reconstruction, and Related Techniques*], Springer Science & Business Media (Dec. 2005).

[3] Reichelt, S., Häussler, R., Fütterer, G., and Leister, N., "Depth cues in human visual perception and their realization in 3d displays," in [*Three-Dimensional Imaging, Visualization, and Display 2010 and Display Technologies and Applications for Defense, Security, and Avionics IV*], **Proc. SPIE 7690**, 76900B–76900B–12 (May 2010).

[4] Häussler, R., Schwerdtner, A., and Leister, N., "Large holographic displays as an alternative to stereoscopic displays," **6803**, 68030M–68030M–9 (2008).

[5] Häussler, R., Reichelt, S., Leister, N., Zschau, E., Missbach, R., and Schwerdtner, A., "Large real-time holographic displays: from prototypes to a consumer product," **7237**, 72370S–72370S–9 (2009).

[6] Häussler, R., Gritsai, Y., Zschau, E., Missbach, R., Sahm, H., Stock, M., and Stolle, H., "Large real-time holographic 3d displays: enabling components and results," *Appl. Opt., AO* **56**, F45–F52 (May 2017).

[7] Reichelt, S., Haussler, R., Leister, N., Futterer, G., Stolle, H., and Schwerdtner, A., "Holographic 3-D Displays - Electro-holography within the Grasp of Commercialization," in [*Advances in Lasers and Electro Optics*], Costa, N. and Cartaxo, A., eds., InTech (Apr. 2010).

[8] Viswanathan, K., Gioia, P., and Morin, L., "A framework for view-dependent hologram representation and adaptive reconstruction," in [*Image Processing (ICIP), 2015 IEEE International Conference on*], 3334–3338, IEEE (2015).

[9] Xing, Y., Pesquet-Popescu, B., and Dufaux, F., "Compression of computer generated phase-shifting hologram sequence using AVC and HEVC," in [*Applications of Digital Image Processing XXXVI*], **Proc. SPIE 8856**, 88561M–88561M–8 (Sept. 2013).

[10] Blinder, D., Bruylants, T., Ottevaere, H., Munteanu, A., and Schelkens, P., "JPEG 2000-based compression of fringe patterns for digital holographic microscopy," *Opt. Eng* **53**, 123102–123102 (Dec. 2014).

[11] Xing, Y., Kaaniche, M., Pesquet-Popescu, B., and Dufaux, F., "Adaptive nonseparable vector lifting scheme for digital holographic data compression," *Appl. Opt., AO* **54**, A98–A109 (Jan. 2015).

[12] Peixeiro, J. P., Brites, C., Ascenso, J., and Pereira, F., "Holographic data coding: Benchmarking and extending hevc with adapted transforms," *IEEE Transactions on Multimedia* **20**(2), 282–297 (2018).

[13] Schretter, C., Bettens, S., Blinder, D., Pesquet-Popescu, B., Cagnazzo, M., Dufaux, F., and Schelkens, P., "Compressed digital holography: from micro towards macro," 99710V–99710V–16, International Society for Optics and Photonics (Sept. 2016).

[14] Darakis, E. and Soraghan, J. J., "Use of Fresnelets for Phase-Shifting Digital Hologram Compression," *IEEE Transactions on Image Processing* **15**, 3804–3811 (Dec. 2006).

[15] Liebling, M., Blu, T., and Unser, M., "Fresnelets: new multiresolution wavelet bases for digital holography," *IEEE Trans Image Process* **12**(1), 29–43 (2003).

[16] Said, A. and Pearlman, W. A., "A new, fast, and efficient image codec based on set partitioning in hierarchical trees," *IEEE Transactions on circuits and systems for video technology* **6**(3), 243–250 (1996).

[17] Viswanathan, K., Gioia, P., and Morin, L., "Wavelet compression of digital holograms: Towards a view-dependent framework," in [*Applications of Digital Image Processing XXXVI*], **Proc. SPIE 8856**, 88561N–88561N–10 (Sept. 2013).

[18] Viswanathan, K., Gioia, P., and Morin, L., "Morlet Wavelet transformed holograms for numerical adaptive view-based reconstruction," in [*Optics and Photonics for Information Processing VIII*], **Proc. SPIE 9216**, 92160G–92160G–14 (Sept. 2014).

[19] El Rhammad, A., Gioia, P., Gilles, A., Cagnazzo, M., and Pesquet-Popescu, B., "Color digital hologram compression based on matching pursuit," *Applied Optics* , 13 (Feb. 2018). Manuscript submitted for publication.

[20] Schwerdtner, A., Leister, N., Häussler, R., Reichelt, S., Fütterer, G., and Schwerdtner, A., "25.2: Eye-Tracking Solutions for Real-Time Holographic 3-D Display," *SID Symposium Digest of Technical Papers* **39**(1), 345–347 (2008).

[21] Takaki, Y. and Okada, N., "Hologram generation by horizontal scanning of a high-speed spatial light modulator," *Appl. Opt., AO* **48**, 3255–3260 (June 2009).

[22] Goodman, J. W., [*Introduction to Fourier Optics*], Roberts and Company Publishers, Englewood, Colo, 3rd ed. (2005).

[23] Lee, T. S., "Image representation using 2d Gabor wavelets," *IEEE Transactions on pattern analysis and machine intelligence* **18**(10), 959–971 (1996).

[24] Mallat, S. G. and Zhang, Z., "Matching pursuits with time-frequency dictionaries," *IEEE Transactions on Signal Processing* **41**, 3397–3415 (Dec. 1993).

[25] Yu, X. and Hu, D., "A Sparse Representation Image Denoising Method Based on Orthogonal Matching Pursuit," *TELKOMNIKA (Telecommunication Computing Electronics and Control)* **13**, 1330 (Dec. 2015).

[26] Rahmoune, A., Vandergheynst, P., and Frossard, P., "MP3d: Highly Scalable Video Coding Scheme Based on Matching Pursuit," ITS Technical Report ITS-TR.06.03, Swiss Federal Institute of Technology EPFL (Nov. 2003).

[27] Needell, D. and Tropp, J. A., "Cosamp: iterative signal recovery from incomplete and inaccurate samples," *Communications of the ACM* **53**(12), 93–100 (2010).

[28] Gilles, A., Gioia, P., Cozot, R., and Morin, L., "Computer generated hologram from Multiview-plus-Depth data considering specular reflections," in [*2016 IEEE International Conference on Multimedia Expo Workshops (ICMEW)*], 1–6 (July 2016).

[29] "Hologram Repository," (2017). https://hologram-repository.labs.b-com.com.

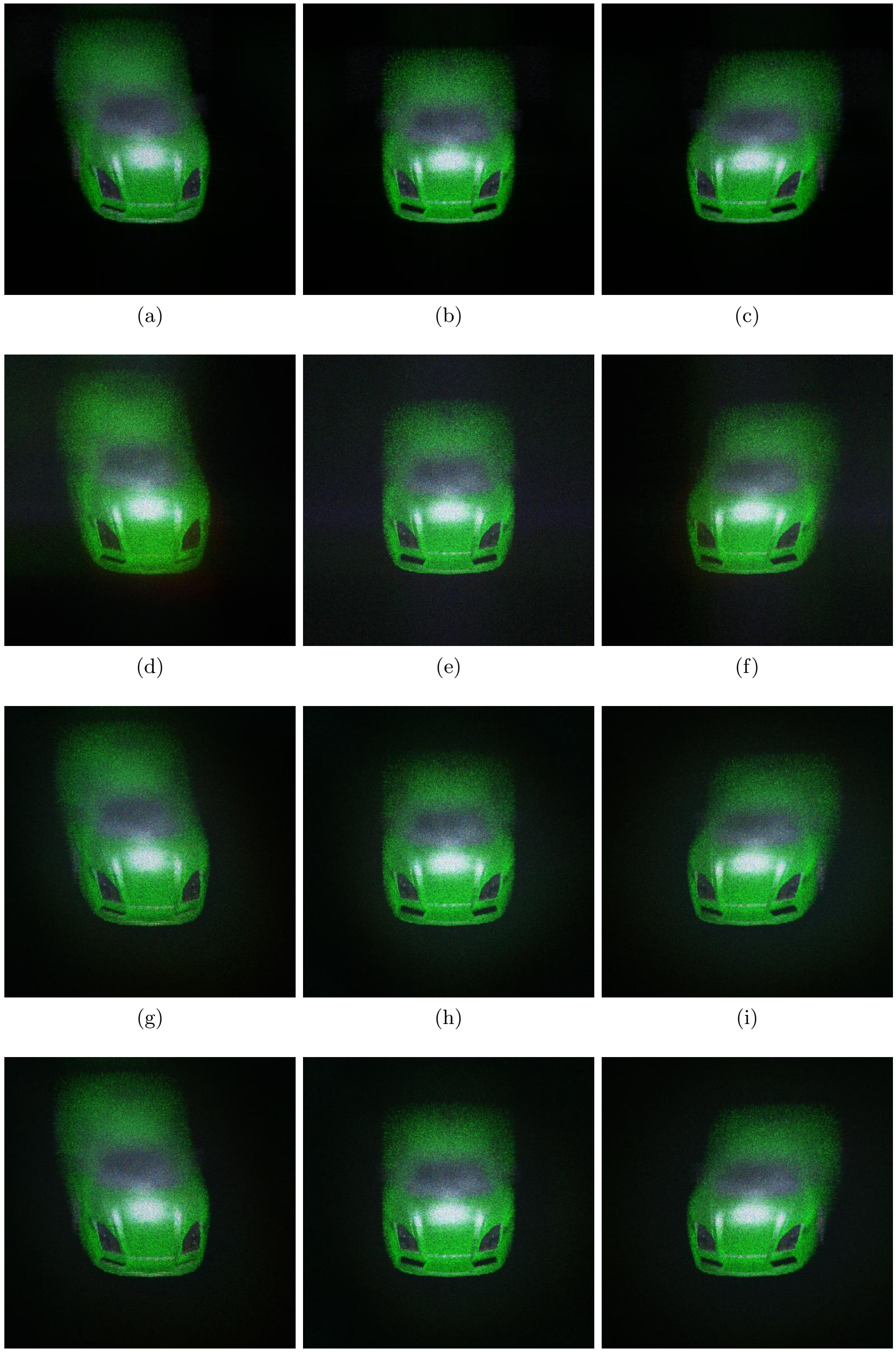

(a) (b) (c) (d) (e) (f) (g) (h) (i) (j) (k) (l)

Figure 6: Reconstructed views of $\mathbf{H}_1$ : (a-c) original, (d-f) HEVC, (g-i) MP-only expansion, (j-l) MP+AS expansion (our approach). The bit-rate for compressed CGH is 2.76 bp

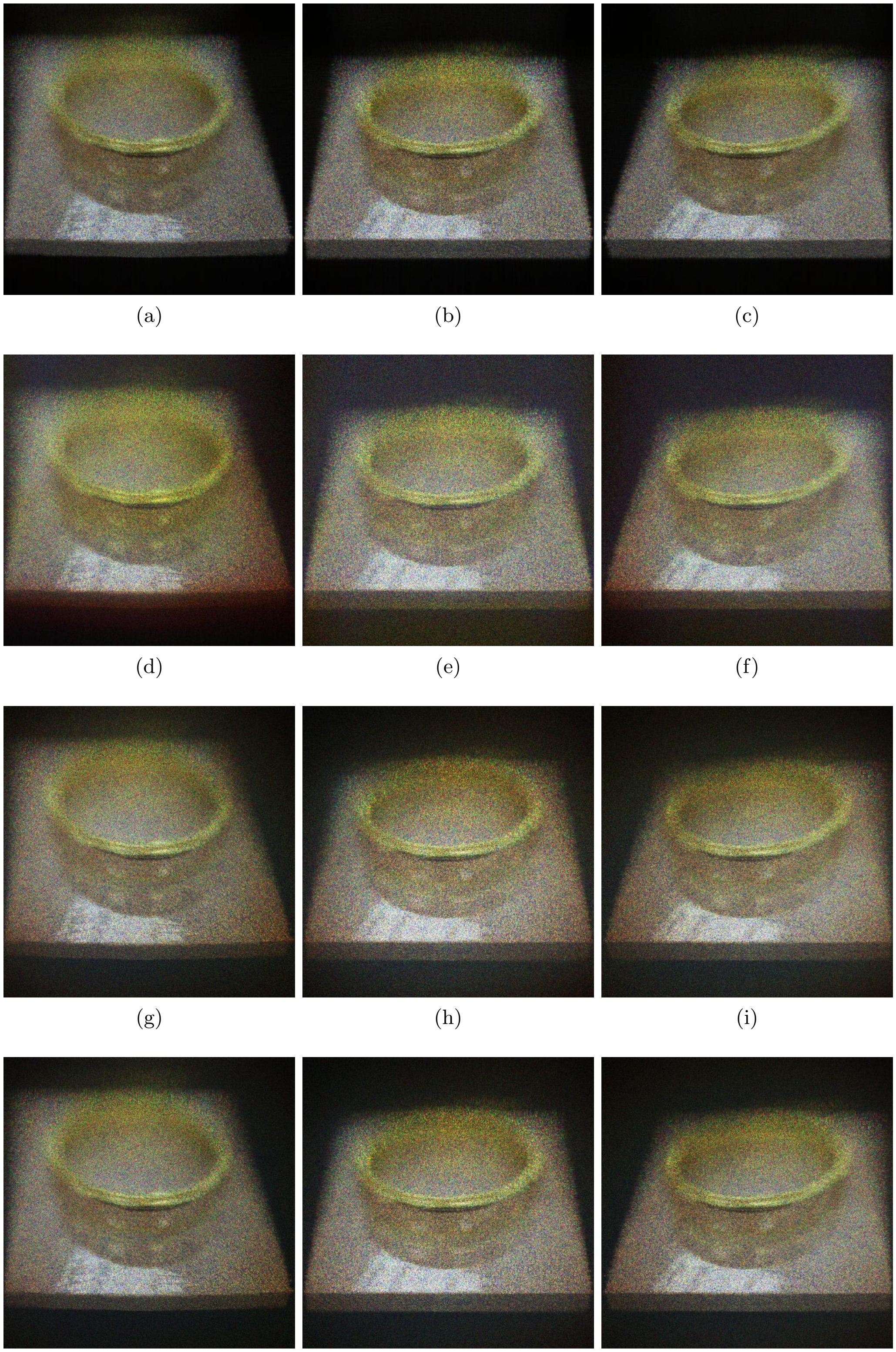

(a) (b) (c)

(d) (e) (f)

(g) (h) (i)

(j) (k) (l)

Figure 7: Reconstructed views of $\mathbf{H}_2$ : (a-c) original, (d-f) HEVC, (g-i) MP-only expansion, (j-l) MP+AS expansion (our approach). The bit-rate for compressed CGH is 2.65 bp